SIF2004 Structural Integrity and Fracture. http://eprint.uq.edu.au/archive/00000836

Simulation Of Crack Trajectories In Materials With Weak Interfaces

A.N. Galybin and A.V. Dyskin

Civil and Resource Engineering, The University of Western Australia, 35 Stirling Highway, Crawley, WA 6009, Australia

ABSTRACT: Propagation of cracks in plane elastic bodies with two mutually orthogonal sets of pre-exiting weak interfaces is studied. It is assumed that crack follows the horizontal interfaces while the vertical ones arrest the crack and produce offsets in the crack path. The method of singular integral equations and the Gauss-Chebyshev quadrature for singular integrals is used with the modification that preserves positions of collocations on every crack segment when crack propagates. The stress intensity factors (SIFs) are calculated for different crack trajectories. Based on these calculations it is found that the preferable crack trajectories are the ones that inclined at an angle to the horizontal direction in which the crack were expected to propagate due to symmetry. One can call this phenomenon the symmetry breaking. The exponent of the power law describing the increase of the mode I SIF with the increasing crack length is close to 0.4 instead of 1/2 for the conventional straight crack.

1 INTRODUCTION

Growing cracks can sometimes follow tortuous paths resulting from combined effects of heterogeneities and pre-existing weak interfaces. The crack propagation is affected by (a) local crack arrest due to the presence of tough inclusions or internal interfaces (e.g., pre-existing fractures) and; (b) non-homogeneity of stress field. The local crack arrest causes abrupt changes in the crack path producing ruptured trajectories in contrast to smoothly fluctuating crack paths associated with the influence of stress non-homogeneity. The stress non-homogeneity alters local principal directions and thus produces fluctuating crack paths [Galybin and Dyskin, 2003]. The present study considers ruptured crack paths caused by internal interfaces in a 2D body. It is assumed that the interfaces are composed of two mutually orthogonal sets of parallel joints as shown in Fig 1. The initial crack is straight and oriented perpendicular to the remote tensile load which is assumed to be insufficient to open the interfaces.

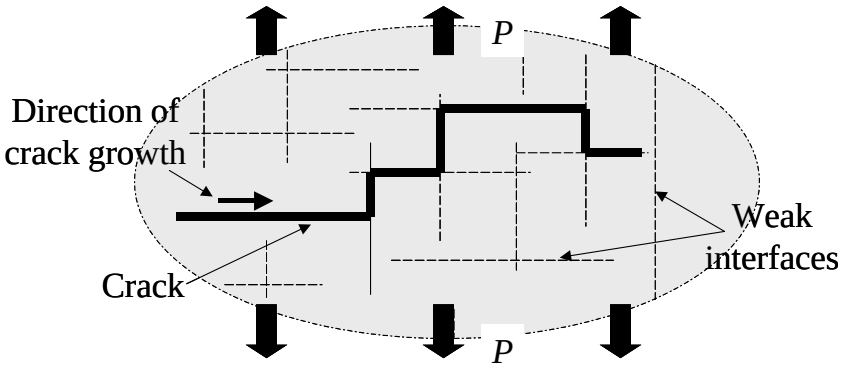

Figure 1 Scheme of crack propagation in a body with internal interfaces

It is assumed that the crack propagates along horizontal interfaces and branches at vertical interfaces as shown in Figure 1. One can relate this mode of crack propagation to the so-called “compressional crossing”, a phenomenon experimentally observed by Renshaw and Pollard [1995] and also in FEM simulations [McConaughy and Engelder, 1999].

2 MATHEMATICAL MODEL

2.1 Singular integral equation (SIE) for polygonal crack

We use an equivalent representation of a curvilinear crack in a plane as a distribution of the displacement discontinuity vector (*u*,*v*) across the crack contour Γ. Then the following singular integral equation, SIE, and the condition of single valuedness of displacements are satisfied to provide equilibrium [Savruk, 1981]

$$\frac{1}{2\pi}\int_\Gamma \left\{\left[\frac{2}{t-t'}+k_1(t,t')\right]Q(t)\,dt+k_2(t,t')\overline{Q(t)\,dt}\right\}=\sigma(t')+i\,\tau(t'),\quad t'\in\Gamma,\qquad \int_\Gamma Q(t)\,dt=0 \tag{1}$$

Here $Q(t)=\dfrac{2G}{1+\kappa}\dfrac{d}{dt}\left[\left(v^+(t)-iu^+(t)\right)-\left(v^-(t)-iu^-(t)\right)\right]$ is unknown complex-valued function unbounded at the ends in which *G* is shear modulus, κ=(3-ν)/(1+ν) for plane stress, κ=3-4ν for plane strain, ν is Poisson's ratio; $\sigma(t')+i\,\tau(t')$ is the stress vector applied to the crack surfaces; *t* and *t'* are complex variables; and regular kernels are given as follows

$$k_1(t,t')=\frac{d}{dt'}\ln\frac{t-t'}{\bar t-\bar t'},\quad k_2(t,t')=-\frac{d}{dt'}\frac{t-t'}{\bar t-\bar t'} \tag{2}$$

Let contour Γ be a polygonal line composed of *N* straight connected segments, Γ_k. (*k=1…N*). Each segment is characterised by a complex coordinate of its centre, χ_k, its half-length L_k, and the angle of inclination, θ_k, to the positive direction of the *x*-axis:

$$\Gamma=\bigcup_{k=1}^{N}\Gamma_k,\quad \Gamma_k=\left\{t_k:\ \ t_k(\eta)=L_k e^{i\theta_k}\eta+\chi_k,\quad |\eta|\le 1\right\} \tag{3}$$

By introducing unknown functions $Q_k(\eta) = Q(t_k(\eta))$ on each segment, eqn (1) can be rewritten as

$$\sum_{k=1}^{N}\frac{L_k}{2\pi}\int_{-1}^{1}\left\{\left[\frac{2}{t_k(\eta)-t'}+k_1(t_k(\eta),t')\right]e^{i\theta_k}Q_k(\eta)+k_1(t_k(\eta),t')e^{-i\theta_k}\overline{Q_k(\eta)}\right\}d\eta=\sigma(t')+i\,\tau(t'),\quad t'\in\Gamma \tag{4}$$

$$\sum_{k=1}^{N}L_k e^{\theta_k}\int_{-1}^{1}Q_k(\eta)\,d\eta=0 \tag{5}$$

Once a solution of (4), (5) is found one can determine the stress intensity factors, K_I and K_{II}, at the left and right ends of Γ from the asymptotics $Q_1(\eta)$ at ηf-1 and $Q_N(\eta)$ at ηf1 respectively.

2.2 Numerical scheme

Since, in general, the solutions of (1) are unbounded at the ends, solutions of (4), (5) are sought as unbounded for the left end of Γ_1 and the right end of Γ_N. Hence solutions on all other segments are bounded. Therefore the functions $Q_k(\eta)$ can be replaced by new regular functions $q_k(\eta)$ as follows

$$Q_1(\eta)=\sqrt{\frac{1-\eta}{1+\eta}}q_1(\eta),\quad Q_k(\eta)=\sqrt{1-\eta^2}\,q_k(\eta),\quad k=2\ldots N-1,\quad Q_N(\eta)=\sqrt{\frac{1+\eta}{1-\eta}}q_N(\eta) \tag{6}$$

After substitution of (6) into (4) and (5) all regular integrals can be calculated in accordance with

the following Gauss-Chebyshev quadratures [Erdogan and Gupta, 1972]

$$\begin{aligned}
&\frac{1}{\pi}\int_{-1}^{1}\frac{(1\pm\xi)q(\xi)}{\sqrt{1-\xi^2}}\,d\xi=\frac{1}{n}\sum_{k=1}^{n}(1\pm\xi_k)q(\xi_k),\quad \xi_k=\cos\frac{2k-1}{2n}\pi,\quad k=1\ldots n\\
&\frac{1}{\pi}\int_{-1}^{1}\sqrt{1-\eta^2}\,q(\eta)\,d\eta=\frac{1}{n}\sum_{j=1}^{n-1}(1-\eta_j^2)q(\eta_j),\quad \eta_j=\cos\frac{j\pi}{n},\quad j=1\ldots n-1
\end{aligned}\tag{7}$$

These formulae are exact if $q(\xi)$ is a polynomial of $(2n\text{-}2)$ degree for the first equation in (7) and of $(2n\text{-}3)$ degree for the second equation.
For singular integrals the Gauss-Chebyshev quadratures have the form

$$\begin{aligned}
&\frac{1}{\pi}\int_{-1}^{1}\frac{1\pm\xi}{\sqrt{1-\xi^2}}\frac{q(\xi)}{\xi-\eta}\,d\xi=\frac{1}{n}\sum_{k=1}^{n}\frac{(1\pm\xi_k)q(\xi_k)}{\xi_k-\eta}+\frac{(1\pm\eta)q(\eta)U_{n-1}(\eta)}{T_n(\eta)}\\
&\frac{1}{\pi}\int_{-1}^{1}\sqrt{1-\eta^2}\,\frac{q(\eta)}{\eta-\xi}\,d\eta=\frac{1}{n}\sum_{j=1}^{n-1}(1-\eta_j^2)\frac{q(\eta_j)}{\eta_j-\xi}-\frac{q(\xi)T_n(\xi)}{U_{n-1}(\xi)}
\end{aligned}\tag{8}$$

Here Chebyshev polynomials

$$T_n(\xi)=\cos(n\arccos\xi),\quad U_{n-1}(\eta)=\sin(n\arccos\eta)\Big/\sqrt{1-\eta^2}\tag{9}$$

have roots ξ_k (k=1…n) and η_j (j=1…n-1) respectively as determined in (7). Formulae (8) are exact if $q(\xi)$ is a polynomial of $(2n\text{-}1)$ or $(2n\text{-}2)$ degrees respectively.
It is obvious that the terms containing Chebyshev polynomials in (8) vanish at the roots of $U_{n-1}(\eta)$ and $T_n(\xi)$. Further ξ_k (k=1…n) are used as collocations for the edge segments and η_j (j=1…n-1) for the internal segments. Although quadratures for each segment have been applied separately based on eqn (4), one can return to the consideration of the original SIE (1) by introducing the following arrays of nodes, collocations and weights

$$\begin{aligned}
X&=\{t_1(\xi_1),\ldots t_1(\xi_n),t_2(\eta_1)\ldots t_2(\eta_{n-1}),\ldots t_{N-1}(\eta_1),\ldots t_{N-1}(\eta_{n-1}),t_N(\xi_1),\ldots t_{N-1}(\xi_n)\}\\
Y&=\{t_1(\eta_1),\ldots t_1(\eta_{n-1}),t_2(\xi_1)\ldots t_2(\xi_n),\ldots t_{N-1}(\xi_1),\ldots t_{N-1}(\xi_n),t_N(\eta_1),\ldots t_{N-1}(\eta_{n-1})\}\\
W&=\{(1-\xi_1)L_1,\ldots(1-\xi_n)L_1,(1-\xi_1^2)L_2\ldots(1-\xi_{n-1}^2)L_2,\ldots\\
&\qquad\ldots(1-\xi_1^2)L_{N-1},\ldots(1-\xi_{n-1}^2)L_{N-1},(1+\xi_1)L_N,\ldots(1+\xi_n)L_N\}
\end{aligned}\tag{10}$$

The number of nodes and weights is $(n\text{-}1)N+2$, the number of collocation is Nn-2. Discretization of (1) leads to the following system of linear algebraic equations

$$\mathbf{AZ}=\mathbf{B},\quad \mathbf{A}=\begin{pmatrix}\mathbf{K}^{11}&\mathbf{K}^{12}\\ \mathbf{K}^{21}&\mathbf{K}^{22}\\ \mathbf{C}&\mathbf{S}\end{pmatrix},\quad \mathbf{B}=\begin{pmatrix}\boldsymbol{\sigma}\\ \boldsymbol{\tau}\\ \boldsymbol{\delta}\end{pmatrix}\tag{11}$$

Here vector $\mathbf{Z}$ represent stacked arrays of real and imaginary parts of unknowns $q_k(\eta)$ in (6) at the nodes; the components of matrixes $\mathbf{K}^{pq}$ ($((n\text{-}1)N+2)\times(Nn\text{-}2)$) ($p$, q=1,2) and vectors $\mathbf{C}$, $\mathbf{S}$, $\boldsymbol{\sigma}$, $\boldsymbol{\tau}$ and $\boldsymbol{\delta}$ have the following form for $l=1\ldots Nn-2$, $m=1\ldots(n-1)N-2$

$$K_{lm}^{11}=\mathrm{Re}\left(K_{lm}^{1}+K_{lm}^{2}\right),\quad K_{lm}^{12}=\mathrm{Re}\left(-iK_{lm}^{1}+iK_{lm}^{2}\right),\quad K_{lm}^{21}=\mathrm{Im}\left(K_{lm}^{1}+K_{lm}^{2}\right),\quad K_{lm}^{22}=\mathrm{Im}\left(-iK_{lm}^{1}+iK_{lm}^{2}\right)$$
$$\sigma_l=\sigma\left(Y_l\right),\quad \tau_l=\tau\left(Y_l\right),\quad C_m=W_m\cos\left(\theta\left(X_m\right)\right),\qquad S_m=W_m\sin\left(\theta\left(X_m\right)\right),\quad \delta_1=0,\quad \delta_2=0 \tag{12}$$
$$K_{lm}^{1}=\frac{W_m}{n}e^{i\left(\theta\left(X_m\right)-\theta\left(Y_l\right)\right)}\mathrm{Re}\left(\frac{e^{i\theta\left(X_m\right)}}{X_m-Y_l}\right),\quad K_{lm}^{2}=\frac{W_m}{2n}\frac{e^{-i\theta\left(X_m\right)}}{\overline{X}_m-\overline{Y}_l}\left(1-\frac{X_m-Y_l}{\overline{X}_m-\overline{Y}_l}e^{-2i\theta\left(Y_l\right)}\right)$$

System (11) is overdetermined if $N>3$ and underdetermined otherwise, therefore the number of segments in polygonal crack is further assumed to be greater than two. The overdetermined system (11) is solved by the least squares method

$$\mathbf{Z}=\left(\mathbf{A}^T\mathbf{A}\right)^{-1}\mathbf{A}^T\mathbf{B} \tag{13}$$

The stress intensity factors, SIFs, at the right/left ends (denoted by superscripts "±" respectively) are calculated as follows

$$K_I^-+iK_{II}^-=2\sqrt{\pi L_1}\,\mathrm{Interp}\left(q_1\left(\xi_j\right),-1\right),\quad K_I^++iK_{II}^+=2\sqrt{\pi L_N}\,\mathrm{Interp}\left(q_N\left(\xi_j\right),1\right) \tag{14}$$

where *Interp*(…,…) denotes the linear interpolation.
The proposed numerical scheme has been verified against known results for branching cracks. It has been found that 4-16 nodes placed on each segment (of equal length) match the accuracy specified in the handbook by Murakami [1987] for different configurations in which the length of the branch and its orientation vary in a wide range. It has been found that more nodes and collocation points are required if the kink is perpendicular to the main crack. Two values (n=8 and n=16) were used in further calculations of the SIFs for perpendicular configurations, however if the difference between the calculated SIFs for 8 and 16 nodes was pronounced, then 32 nodes were used to refine calculations.

3 SIMULATION OF CRACK GROWTH IN FRAGMENTED 2D PLATE

A crack approaching a weak interface (Figure 2a) generates delaminating and sliding zones on the interface ahead of the crack tip [e.g. Parton, 1992].

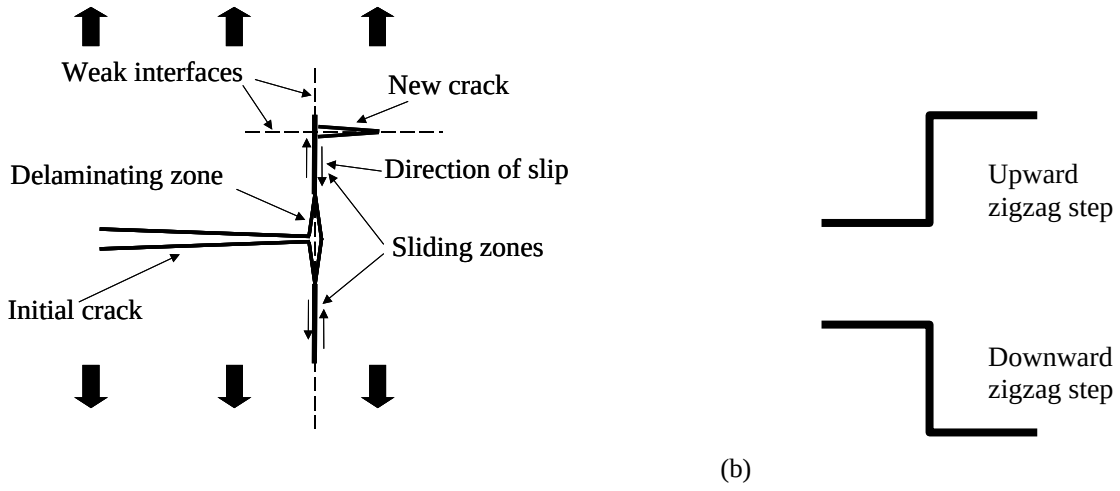

Figure 2. Crack propagation through the interface: (a) generation of delaminating and sliding zones and a new crack; (b) an elementary zigzag step of crack propagation each segment having the length equal to 2.

Calculations show that the size of delaminating zone is small compared to the length of the initial horizontal crack. Thus, if the delaminating zone is associated with the kink of the branching crack

(Fig 2a) then calculations demonstrate that K_I at the kink tip is negative provided that the kink is 10 (or less) times shorter than the initial crack. At the same time the length of the sliding zone can be comparable with the length of the initial crack and it can reach the nearest horizontal interface. Therefore a new crack can be induced in the horizontal direction by the tensile stresses acting near the end of the sliding zone. When this new crack approaches the next vertical interface another step-crack can be generated upwards or downwards and so on. Therefore, the process of crack growth can be viewed as a sequence of elementary zigzag steps shown in Figure 2b. The described mechanism of crack propagation is the further development of the concept of "compressional crossing" [Renshaw and Pollard, 1995].

3.1 Possible configurations of the trajectory of crack propagation

As evident from Figure 2, the crack propagation through materials with multiple weak interfaces is characterised by the offsets along the interface. In the case of a system of parallel interfaces the crack path will consist of elementary zigzag steps. Now we analyse the SIFs for different sequences of zigzag steps in order to reveal the most probable paths of crack propagation. The applied load is assumed to be equal to 1 unit. It is assumed that the priority of up- or downward steps in the crack path is controlled by the largest mode I SIF calculated after each possible zigzag step from the left/right tip of the crack. Figure 3 shows values of the dimensionless SIFs (see the expression at the top of Figure 3) at each crack tip for different crack paths. In all configurations the total length of the cracks (including vertical segments) is L=20. It is seen that the trajectories with offsets in the same direction (cases *a*, *b*, *c* and *d*) are more preferable, because of higher SIFs, than the trajectories with alternating offset directions (cases *e* and *f*).

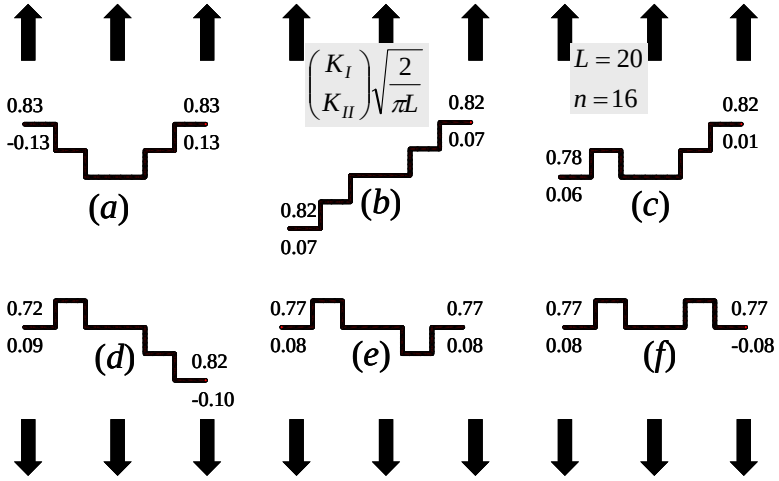

Figure 3 Stress intensity factors (SIFs) for different configurations: the numbers correspond to dimensionless SIFs (mode I above mode II); the applied load is assumed equal to 1unit.

3.2 Stress intensity factor vs. crack length

Based on the previous analysis two crack paths are investigated in this subsection. They represent the most (Figure 3b) and least (Figure 3f) preferable paths. In both these cases each segment has unit half-length and the initial crack consists of two segments. The maximum length of the crack is L=20. For the case of vertical load applied at infinity the mode I SIF is a square root function of the crack length for a straight crack propagating through the material, $K_I=\sigma_0(\pi L/2)^{1/2}$. In the cases considered here the SIFs increase weaker than the square root. The results of calculation of the SIFs (doted curves) and fitting by power functions (solid lines in Figure 4*b, d*) are shown together with the square root dependence (dash-dot curve) and the special dependence $K_I=\sigma_0(\pi\Lambda/2)^{1/2}$ (dash

curve) where the effective crack length Λ is the projection of the crack onto horizontal axis.
Also, several cases in which the crack path is random have been investigated. The paths have been specified by random up- or downward zigzag steps. The results of fitting of the calculated SIFs to the power law have shown that the exponent is less than ½ for all analysed cases. This suggests that the power law with the exponent smaller than ½ correctly describes the behaviour of the mode I SIF in random propagation of the crack through the fractured material.

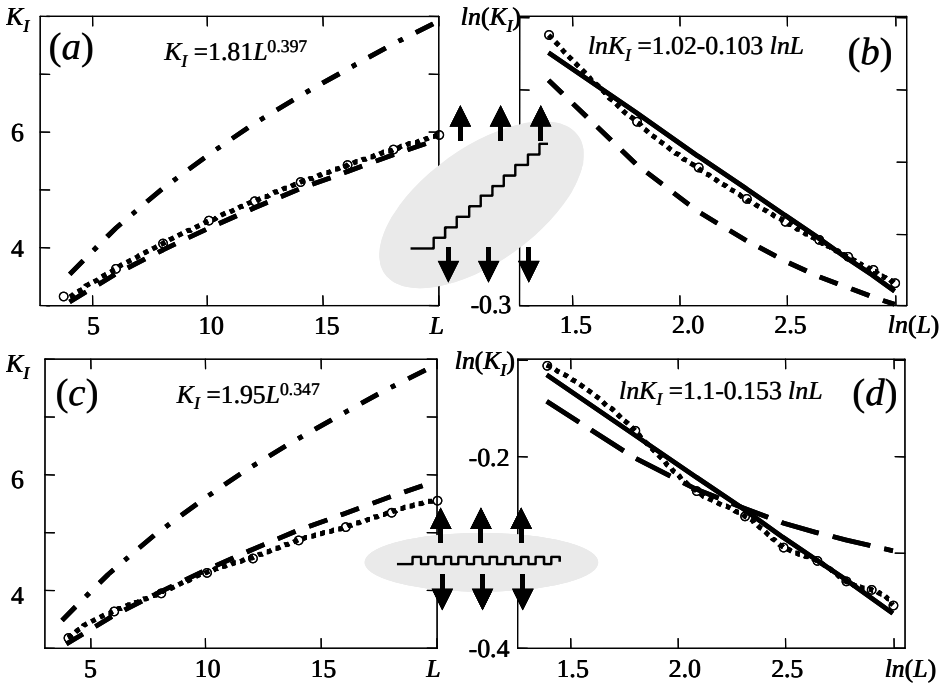

Figure 4 Mode I SIFs vs. length: the dotted lines show the calculated values; the dash-dotted lines show the case of straight crack with the same total length as the cracks considered; the broken line show the case of straight crack with the total length equal to the projection of the cracks considered on the *x*-axis; the solid lines on log-log graphs show the linear regression

4 CONCLUSIONS

The analysis shows that the preferable crack trajectories are the ones that inclined at an angle to the horizontal direction in which the crack were expected to propagate due to symmetry. One can call this phenomenon the symmetry breaking. The exponent of the power law describing the increase of K_I with the increasing crack length is close to 0.4 in contrast to 1/2 for the straight crack.

REFERENCES

Erdogan F. and G.D. Gupta. On the numerical solution of singular integral equations, *Quart. Appl. Math*. **29** (1972) pp. 525-534.

Galybin, A.N. and A.V. Dyskin. Random trajectories of crack growth caused by spatial stress fluctuations. *International Journal of Fracture*. (2004) In print.

McConaughy, D.T. and T. Engelder. Joint interaction with embedded concretions: joint loading configurations inferred from propagation paths. *Journal of Structural Geology* **21**, (1999) pp. 1637-1652.

Murakami, Y. *Stress Intensity Factors Handbook 1*, Pergamon Press, Oxford, New York (1987).

Parton, V.Z., *Fracture Mechanics. From Theory to Practice*. Gordon and Breach Science Publishers, Philadelphia (1992).

Renshaw, C.E. and D.D. Pollard. An experimentally verified criterion for propagation across unbounded frictional interface in brittle, linear elastic materials. *Intern. J. Rock Mech. Mining Sci.* **32** (1995) pp 237-249.

Savruk, M. P. *Two-Dimensional Problems of Elasticity for Body with Cracks*, Naukova Dumka, Kiev, (1981)